

Structural optimization of the low-pressure Venturi injector with double suction ports based on computational fluid dynamics and orthogonal test

Lei Zhang*, Zhengying Wei, Qian Zhang

The State Key Laboratory for Manufacturing Systems Engineering, Xi'an Jiaotong University, Xi'an 710049, China, Tel. +86-29-8266-5064/+86-21-8266-5064; Fax: +86-29-8266-9046; email: zl870127@stu.xjtu.edu.cn (L. Zhang), Tel. +86-21-8266-9046; email: zywei@mail.xjtu.edu.cn (Z.Y. Wei), Tel. +86-21-8266-5064; email: jerryz2017@stu.xjtu.edu.cn (Q. Zhang)

Received 22 May 2020; Accepted 25 October 2020

ABSTRACT

In the low-pressure irrigation system, a Venturi injector of low working pressure and energy consumption with a double-suction port was designed. The computational fluid dynamics method was used to simulate the inner flow field of Venturi injectors to obtain hydraulic performances. Taking the fertilizer mixing concentration as the evaluation index, an orthogonal test of six factors and five levels was designed to acquire the optimal structure with numerical calculation. The parameters in the optimal structure were as follows: the convergence angle 24° , the throat contraction ratio 0.2, the throat length-diameter ratio 2.0, the expanding angle 6° , the inclination angle 50° , and the number of suction port 2. Compared with the Venturi injector with a single suction port of inclination angle 90° , fertilizer suction discharge and mixing concentration of the double-suction port structure were increased by 236% and 198.8%, respectively. The double-suction port structure with an inclination angle 50° has better performances, including lower starting working pressure, more fertilizer suction discharge and mixing concentration, and is suitable for the low-pressure irrigation system.

Keywords: Venturi injector; Low-pressure irrigation system; Computational fluid dynamics; Injection performance; Orthogonal test

1. Introduction

With the rapid development of agricultural modernization, automatic fertigation is applied in field crops, facility agriculture, horticulture, and vegetable greenhouse [1]. Various fertilizer injection units, such as self-pressured injecting device, pressure differential fertilizer tank [2], proportional injection pump, automatic fertilizing machine [3] and Venturi injector [4], are used in the integrated water-fertilizer irrigation [5]. The performance of the fertilizer injector unit has a great impact on the fertilizer suction amount and the water-fertilizer mixing uniformity. Venturi injector is widely used in fertigation system due to the significant advantages of convenient operation, low cost, easy installation, and effective work without extra power.

However, the Venturi injectors on the market have several problems as follows:

- Starting working pressure of the Venturi injector is more than 0.1 MPa, so a high-lift pump should be installed at the head part of the irrigation system to provide high pressure.
- Unstable performance results in the uneven mixing of water and fertilizer, thus crops cannot get enough fertilizer [6,7].
- Size is large so as to install in greenhouses difficultly.

Low-pressure irrigation [8,9] is a new model that optimizes energy distribution and reduces energy loss when considering different terrain. The saving efficiency of

* Corresponding author.

water and fertilizer is more than 80% [10,11]. Therefore, it is necessary to design a Venturi injector suitable for the low-pressure irrigation system and the existing defects are improved. Now, most studies about Venturi injectors only focus on performance parameters from experimental tests [12,13]. The experimental method is time-consuming and high cost because a lot of Venturi injectors are fabricated, installed, and tested. Computational fluid dynamics (CFD) [14] is a high-efficiency method to research hydraulic performances. This method is used to simulate the inner flow field and get the performance parameters of Venturi injectors. Combined with the orthogonal test, the comprehensive effect of structural parameters on performance and the optimal structure are acquired.

2. Design and methods

2.1. Structure and principle of Venturi injector

A typical structure of the Venturi injector was designed as shown in Fig. 1. It includes inlet section L_1 , contraction segment L_2 , throat section L_3 , divergent segment L_4 , outlet section L_5 , and suction port section L_6 . The working principle is based on the Venturi effect [15,16]. When the pressure water flows through the inner cavity of the Venturi tube, the velocity becomes larger due to the shrinking diameter to bring about negative pressure in the throat section. Under atmospheric pressure, the fertilizer is inhaled into the Venturi tube.

2.2. Experimental facility

The schematic diagram of the experimental device is illustrated in Fig. 2. The pipes were all made of polyvinyl chloride. The main pipe had a diameter of 40 mm, the pipe diameter connected with the inlet and outlet of the Venturi injector was 20 mm. To measure the discharges of the inlet, outlet, and suction port, three turbine flow meters (Zhongjiang, Foshan, China) with an accuracy of $\pm 5\%$ were installed upstream of the inlet and suction port and downstream of the outlet. Two pressure gauges (0.4 MPa, Hakin, Qingdao, China) with 2.5% precision were installed to detect the inlet and outlet pressure of the Venturi injector. The different inlet pressures were supplied using the

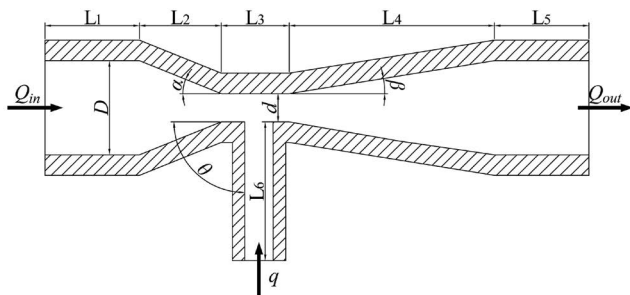


Fig. 1. Structure of Venturi injector. Q_{in} inlet discharge; D diameter of inlet and outlet; α convergence angle of contraction segment; d diameter of throat section; β expanding angle of divergent segment; Q_{out} outlet discharge; θ inclination angle of suction port; q fertilizer suction discharge.

variable frequency pump (XKJ-804S, LEO, Wenling, China). The outlet pressure was regulated by a ball valve. The liquid fertilizer was replaced by clean water in the fertilizer tank. The vertical distance between the water level and the suction port was kept constant with a value of 50 ± 10 mm.

2.3. Experimental settings

The inlet pressure p_1 was set as 0.05 and 0.1 MPa. The outlet pressure p_2 was set as 0, 0.01, 0.02, 0.03, 0.04, 0.05 MPa. The inlet pressure p of the suction port was set as 0 MPa.

Under various conditions, the fertilizer suction discharge q was recorded and the fertilizer mixing concentration ζ (the ratio of fertilizer suction discharge q to outlet discharge Q_{out}) was calculated. All experimental data were recorded under stable pressures for 1 min and each condition was repeated three times. The structural parameters are shown in Table 1.

2.4. CFD method

CFD is a convenient method for the analysis of single-phase and multi-phase fluid states. The hydraulic performance of the Venturi injector was simulated by Fluent 15.0. In Table 2, the average Q_{in} (the difference between Q_{out} and q) was about 900 L/h. The average inlet flow rate v was 1.244 m/s as shown in Eq. (1). In the experiment, the liquid was clean water. So, the fluid kinematic viscosity was 1.0574×10^{-6} m²/s at 18°C. The Reynolds number Re was 18,823 (more than 4,000) as shown in Eq. (2), hence the inner flow field belonged to the turbulence model. The standard $k-\epsilon$ turbulence model was selected to represent the flow field of the Venturi injector [17–19]. The first-order upwind scheme and the classic simple algorithm were set to solve the governing equations. All convergent values were set to less than 10^{-4} . The three-dimensional mesh model of the Venturi injector was established by Workbench 15.0. The unstructured grids with a size of 1 mm were used.

$$v = \frac{Q_{in}}{\pi R^2} = \frac{4Q_{in}}{\pi D^2} \quad (1)$$

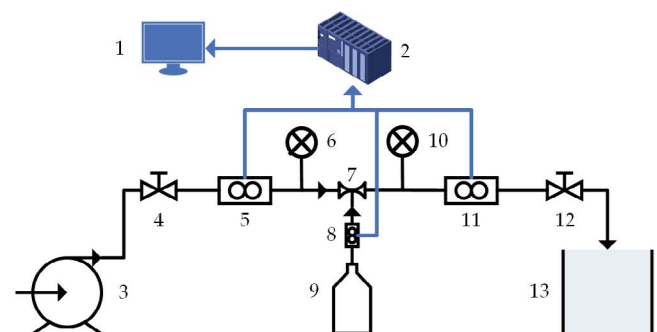


Fig. 2. Schematic diagram of experimental platform for Venturi injector: 1 = computer; 2 = S7-200 PLC controller; 3 = variable frequency pump; 4 = inlet control valve; 5 = inlet flow meter; 6 = inlet pressure gauge; 7 = Venturi injector; 8 = suction port flow meter; 9 = fertilizer tank; 10 = outlet pressure gauge; 11 = outlet flow meter; 12 = outlet control valve; 13 = mixing tank of water and fertilizer.

Table 1
Structural parameters of the Venturi injector

Parameter	Value
Inlet and outlet diameter D (mm)	16
Convergence angle α (°)	16, 18, 20, 22, 24, 26, 28, 30, 32
Contraction ratio of throat κ^a	0.15, 0.20, 0.25, 0.30, 0.35, 0.40, 0.45, 0.50
Throat length-diameter ratio γ^b	1.2, 1.4, 1.6, 1.8, 2.0, 2.2, 2.4, 2.6, 2.8
Expanding angle β (°)	4, 5, 7, 9, 11, 13, 15
Inclination angle θ (°)	40, 50, 60, 70, 80, 90
Number of suction ports n	1, 2, 3, 4

^aratio of throat diameter d to inlet diameter D ;

^bratio of throat length L_3 to throat diameter d .

Table 2
Simulated and experimental data under gradient pressure difference

p_1 (MPa)	p_2 (MPa)	q (L h ⁻¹)			Q_{out} (L h ⁻¹)			ζ		
		Sim. ^a	Exp. ^b	Err. ^c (%)	Sim.	Exp.	Err. (%)	Sim.	Exp.	Err. (%)
0.1	0	120.96	114.48	5.66	1,116.24	1,155.43	-3.39	10.84	9.91	9.37
0.1	0.01	102.46	93.99	9.01	1,091.84	1,077.74	1.31	9.38	8.72	7.60
0.1	0.02	86.56	87.02	-0.53	1,071.46	1,060.29	1.05	8.08	8.21	-1.57
0.1	0.03	67.13	66.63	0.75	1,045.86	1,023.53	2.18	6.42	6.51	-1.40
0.1	0.04	46.31	47.36	-2.21	1,022.26	999.14	2.31	4.53	4.74	-4.43
0.1	0.05	14.4	15.78	-8.74	989.02	984.12	0.50	1.46	1.60	-9.20

^asimulation value;

^bexperiment value;

^cerror (the percentage error between the simulated and experimental values).

$$Re = \frac{\rho v D}{\eta} = \frac{\rho v D}{\mu \rho} = \frac{v D}{\mu} \quad (2)$$

2.5. CFD verification

The parameters of the initial structure are: D 16 mm, α 22°, κ 0.3, γ 2.0, β 7°, θ 90°, n 1. The boundary conditions were set as p_1 0.1 MPa and p_2 0, 0.01, 0.02, 0.03, 0.04, and 0.05 MPa.

Under the same working conditions, q and Q_{out} can be obtained by CFD. Then ζ was calculated. All data are shown in Table 2. Each error between simulation and experiment is less than 10%. Hence, this solution approach is reasonable. It can be used to analyze the practical performance of the Venturi injector.

2.6. Structural optimization

The structure (Table 1) in the range of each parameter was simulated to obtain the trend charts (Fig. 3) of q and ζ . The boundary conditions were: p_1 0.1 MPa; p_2 0 MPa.

Fig. 3a shows that q and ζ increase first and then decrease rapidly as α increases. q and ζ keep stable values in the range of 18°–26°. In Fig. 3b q increases with the increase of κ , but the trend of ζ is the opposite.

Fig. 3c illustrates q and ζ raise gradually as γ increases. In Figs. 3d and e when β and θ increase, q and ζ reduce

simultaneously. Fig. 3f indicates that q and ζ enhance significantly with more than one suction port and the Venturi injectors with even numbers of suction ports have better performances. Taking fabrication and structural interference into consideration, the optimal values of α , κ , γ , β , θ , n are 18–26, 0.2–0.4, 1.6–2.4, 5–9, 50–90, 2, respectively.

CFD method improves the disadvantages of the experimental method, but it takes a lot of time when a large number of structures are simulated. The orthogonal test method [20] can be used to reduce the number of structures and find the optimal combination structure. According to the number of parameters and their optimal range, a six-factor and five-level L_{25} (5^6) orthogonal table was designed with a blank term [21,22] regardless of the interaction between the parameters. The levels of each parameter are shown in Table 3.

The orthogonal test table has 25 parameter combinations, which are simulated under the condition of p_1 0.05 MPa and p_2 0 MPa. ζ calculated is used as the evaluation index of Venturi injector in orthogonal tests. So, the orthogonal tests and the index are shown in Table 4.

From Table 4, the five values of ζ corresponding to level i ($i = 1, 2, 3, 4, 5$) of each factor were summed to get K_i . k_i was the mean of K_i . Then the intuitive data can be obtained to establish in Table 5. k_i represents the ζ of level i of each parameter.

The trend chart of the influence of every parameter on ζ (k in Table 5) is shown in Fig. 4. ζ decrease with the increase

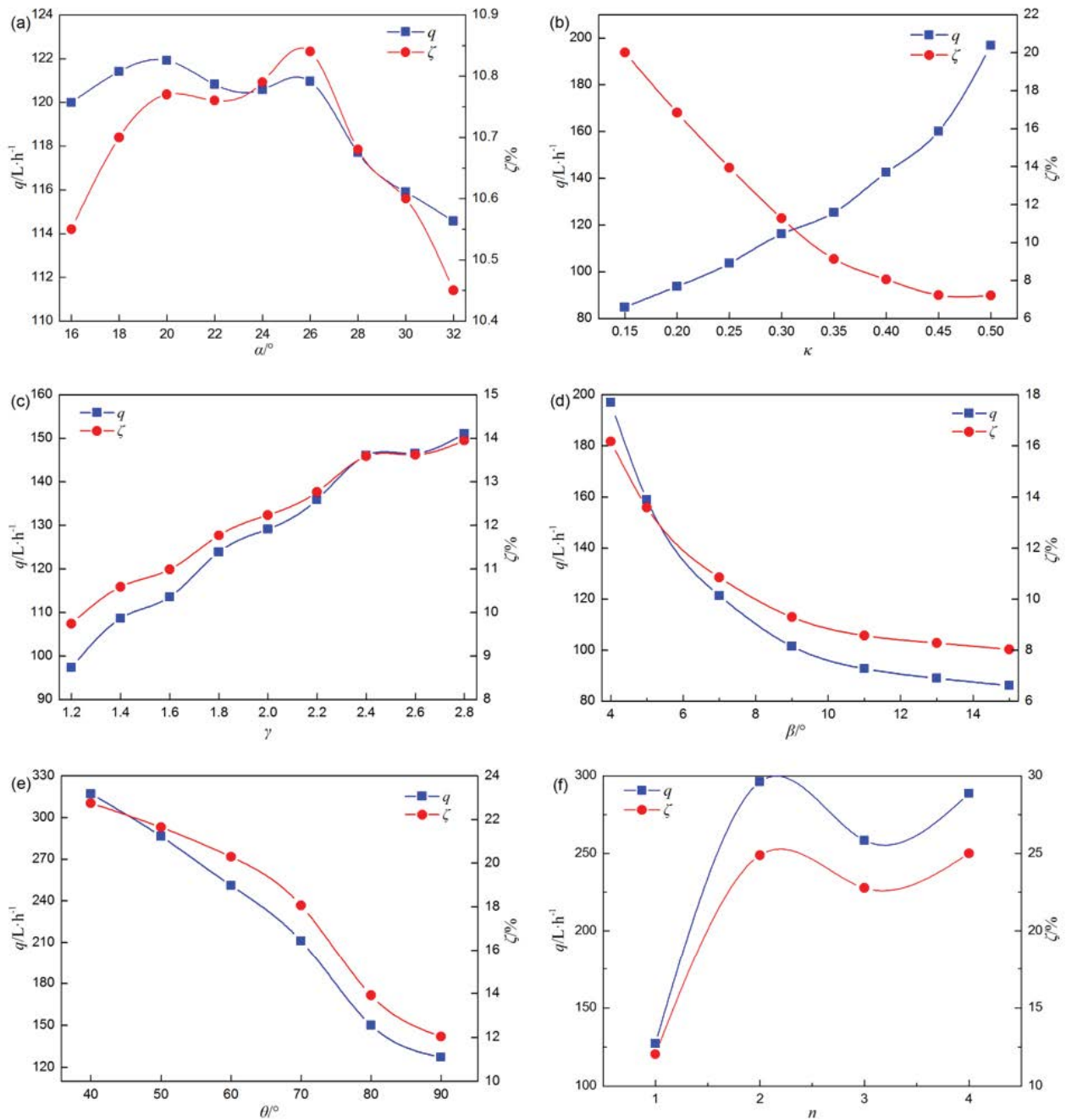


Fig. 3. Relationship between q , ζ and (a) α , (b) κ , (c) γ , (d) β , (e) θ and (f) n .

Table 3
Factors and levels of $L_{25} (5^6)$ orthogonal test

Factor	Level 1	Level 2	Level 3	Level 4	Level 5
α ($^\circ$)	18	20	22	24	26
κ	0.2	0.25	0.3	0.35	0.4
γ	1.6	1.8	2	2.2	2.4
β ($^\circ$)	5	6	7	8	9
θ ($^\circ$)	50	60	70	80	90

of κ and θ , and fluctuate with the increase of α , γ , and β . The optimal combination for the maximum ζ is $\alpha = 24^\circ$, $\kappa = 0.2$, $\gamma = 2.0$, $\beta = 6^\circ$, $\theta = 50^\circ$. However, this combination does not exist in the orthogonal test. The new structure will be analyzed to know the performance.

3. Results and discussion

3.1. Influence of parameter on fertilizer mixing concentration

R_d (the difference between the maximum and minimum k (Table 5) of each factor) presents the effect of structural

Table 4
L₂₅ (5⁶) orthogonal test and results

Sequence	α (°)	κ	γ	β (°)	θ (°)	Blank	ζ (%)
1	18	0.20	1.60	5	50	1	30.53
2	18	0.25	1.80	6	60	2	30.58
3	18	0.30	2.00	7	70	3	25.85
4	18	0.35	2.20	8	80	4	20.76
5	18	0.40	2.40	9	90	5	16.13
6	20	0.20	1.80	7	80	5	25.15
7	20	0.25	2.00	8	90	1	21.56
8	20	0.30	2.20	9	50	2	29.28
9	20	0.35	2.40	5	60	3	31.23
10	20	0.40	1.60	6	70	4	24.84
11	22	0.20	2.00	9	60	4	28.35
12	22	0.25	2.20	5	70	5	28.19
13	22	0.30	2.40	6	80	1	25.61
14	22	0.35	1.60	7	90	2	16.96
15	22	0.40	1.80	8	50	3	13.29
16	24	0.20	2.20	6	90	3	27.60
17	24	0.25	2.40	7	50	4	31.55
18	24	0.30	1.60	8	60	5	27.83
19	24	0.35	1.80	9	70	1	21.13
20	24	0.40	2.00	5	80	2	24.55
21	26	0.20	2.40	8	70	2	27.02
22	26	0.25	1.60	9	80	3	19.85
23	26	0.30	1.80	5	90	4	24.17
24	26	0.35	2.00	6	50	5	32.89
25	26	0.40	2.20	7	60	1	16.39

Table 5
Intuitive analysis of fertilizer mixing concentration

	α (°)	κ	γ	β (°)	θ (°)
K_1	123.85	138.65	120.01	138.67	137.54
K_2	132.06	131.73	114.32	141.52	134.38
K_3	112.40	132.74	133.20	115.90	127.03
K_4	132.66	122.97	122.22	110.46	115.92
K_5	120.32	95.20	131.54	114.74	106.42
k_1	24.77	27.73	24.00	27.73	27.51
k_2	26.41	26.35	22.86	28.30	26.88
k_3	22.48	26.55	26.64	23.18	25.41
k_4	26.53	24.59	24.44	22.09	23.18
k_5	24.06	19.04	26.31	22.95	21.28

parameters on ζ . Fig. 5 shows that the impact of structural parameters is $\kappa > \theta > \beta > \alpha > \gamma$. κ is the most relevant parameter for the performance of the Venturi injector. It is consistent with the Venturi effect. θ changes the direction of fertilizer flow to affect the mixed state between fertilizer and water. β represents the size of the water-fertilizer mixing space. α and γ on performance are not significant and can be ignored. These results provide references for the structural design of the Venturi injector.

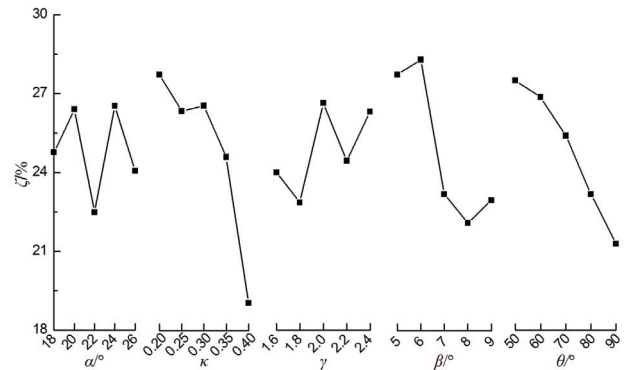


Fig. 4. Trend chart of fertilizer mixing concentration influenced by five structural parameters.

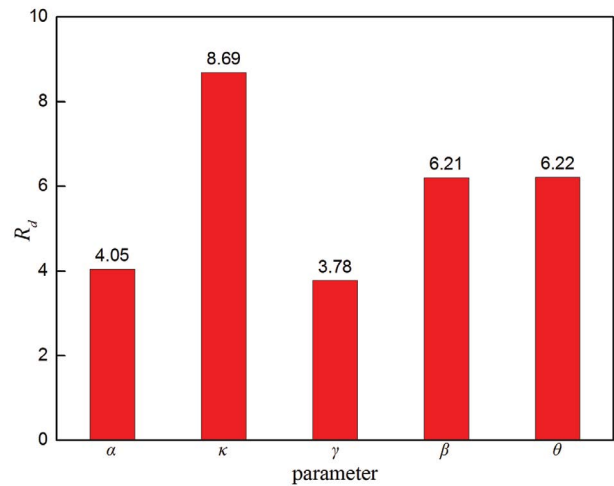


Fig. 5. R_d of five factors: α , κ , γ , β , θ .

3.2. Comparison of initial and optimized structure

Under the same boundary conditions of p_1 0.01, 0.02, 0.03, 0.04, 0.05, and p_2 0 MPa, the inner flow field of the initial and optimized structure was simulated. The results about q and ζ are shown in Table 6. q and ζ increase by more than 210% and 190%, respectively.

In addition to the intuitive performance parameters, the characteristics of the internal flow field also play a significant role in water-fertilizer mixing uniformity and working stability. The axial cross-section of three-dimensional simulation results is extracted. The pressure distribution diagram and velocity streamline diagram can be obtained as shown in Figs. 6 and 7.

Fig. 6a indicates that the negative pressure zone is located in the throat section behind the suction port and extends to the divergent segment. The minimum negative pressure is concentrated on the pipe wall at the junction of the throat section and the divergent segment. Extremely uneven distribution of negative pressure may cause instability of fertilizer suction, even be unworkable. After optimization, the negative pressure zone is distributed in the

Table 6
Performance comparison between the initial and optimized structure

p_1 (MPa)	p_2 (MPa)	q (L h ⁻¹)			ζ (%)		
		Initial structure	Optimized structure	Performance improvement (%)	Initial structure	Optimized structure	Performance improvement (%)
0.01	0	24.49	77.32	215.72	6.23	18.90	203.37
0.02	0	44.65	148.32	232.18	8.50	25.43	199.18
0.03	0	59.37	204.80	244.96	9.42	28.35	200.96
0.04	0	71.52	245.27	242.94	9.93	29.38	195.87
0.05	0	81.52	280.40	243.96	10.19	30.02	194.60

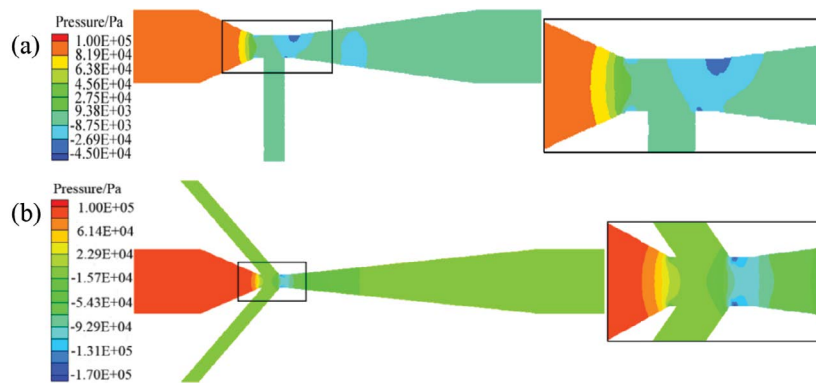


Fig. 6. Pressure distribution of initial and optimized structure: (a) initial structure and (b) optimized structure.

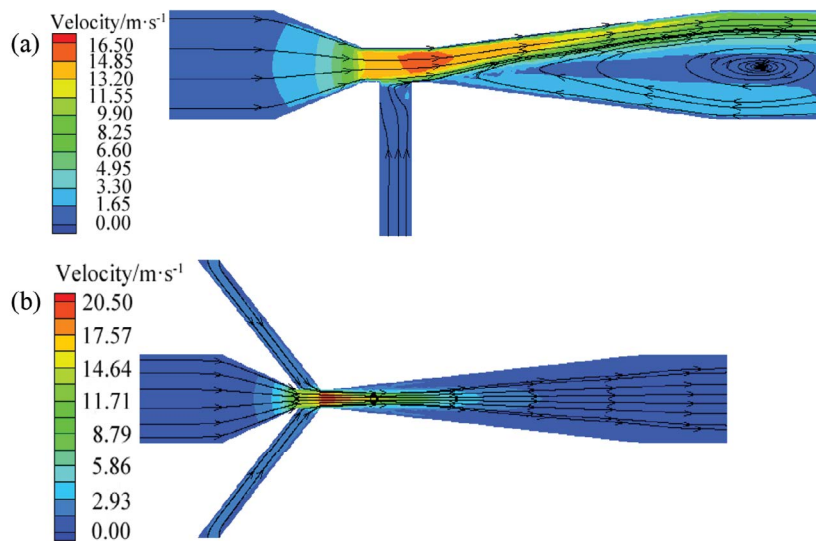


Fig. 7. Velocity streamline of initial and optimized structure: (a) initial structure and (b) optimized structure.

throat section behind suction ports evenly. The position of minimum negative pressure moves forward and is concentrated on the pipe wall at the junction of the throat section and suction ports as shown in Fig. 6b. In consequence, the stability is improved and the start-up working pressure is reduced.

Fig. 7a represents that there is a large vortex in the lower part of the divergent segment and outlet section and

the fertilizer is mixed with water only in a small area at the upper part of the divergent segment. The vortex results in energy loss. Moreover, only a small amount of fertilizer can be suctioned into the throat section. These phenomena will affect the uniformity of fertilizer concentration. Fig. 7b shows that the fertilizer is completely inhaled into the throat section through the two suction ports. There are only small vortices near the pipe wall of the divergent

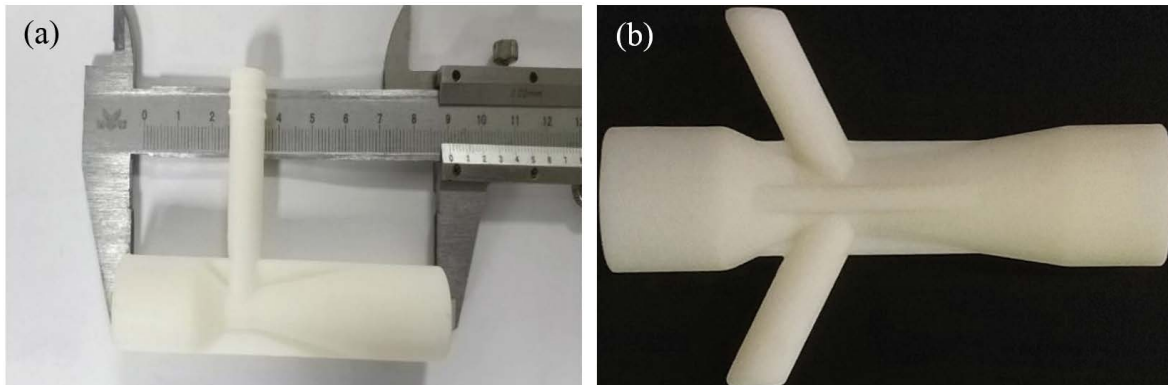


Fig. 8. Prototype of Venturi injector: (a) initial structure and (b) optimized structure

segment. In the divergent segment, the water and fertilizer are mixed sufficiently.

Compared with the initial structure, stability and uniformity are greatly improved after optimization. Under the inlet pressure of less than 0.05 MPa, q and ζ increase by an average of 235.95% and 198.80%, respectively. Because the low inlet pressure enables the optimized Venturi injector to suction fertilizer for high-quality work, it is more suitable for the low-pressure irrigation system. The optimized prototype of the Venturi injector is fabricated using 3D printing (Fig. 8b). The stiffeners are designed on the outside of the throat section to enhance the strength of the overall structure. The new Venturi injector can complete the integrated water-fertilizer irrigation.

4. Conclusion

Instead of the experimental method, the CFD and orthogonal test methods could reduce the fabrication cost, installation and test time. Compared with the Venturi injector with only one suction port (inclination angle 90°), the fertilizer suction discharge and mixing concentration of the optimized structure were increased by 235.95% and 198.80%, respectively. The fertilizer mixing concentration was up to 20%, so it ensured the fertilizer supply needed by crops. In the inner flow field of optimized structure, the negative pressure zone was distributed in the throat section behind suction ports evenly and there were only small vortexes near the pipe wall of the divergent segment. Hence the stability of suction fertilizer and the uniformity of fertilizer mixing concentration were better. The Venturi injector with double-suction ports (inclination angle 50°) had low working pressure to reduce the energy demands of the irrigation system, so it was suitable for a low-pressure irrigation system.

Symbols

D	—	Diameter of inlet and outlet, m
d	—	Diameter of throat section, m
n	—	Numbers of the suction port
p	—	Pressure of suction port, MPa
p_1	—	Inlet pressure, MPa
p_2	—	Outlet pressure, MPa

q	—	Fertilizer suction discharge, L/h
Q_{in}	—	Inlet discharge, L/h
Q_{out}	—	Outlet discharge, L/h
R	—	Inlet radius, m
Re	—	Reynolds number
v	—	Fluid velocity, m/s
α	—	Convergence angle of contraction segment, $^\circ$
β	—	Expanding angle of the divergent segment, $^\circ$
γ	—	Throat length-diameter ratio
ζ	—	Fertilizer mixing concentration, %
η	—	Fluid dynamic viscosity, Pa·s
θ	—	Inclination angle of suction port, $^\circ$
κ	—	Contraction ratio of throat
μ	—	Fluid kinematic viscosity, m^2/s
ρ	—	Fluid density, kg/m^3

Acknowledgment

The authors would like to acknowledge the financial support from the National Key Research and Development Plan of China (No.2016YFC0400202).

References

- [1] S.R. Evett, T.A. Howell, A.D. Schneider, D.R. Upchurch, D.F. Wanjura, Automatic Drip Irrigation of Corn and Soybean, Proceedings of the 4th Decennial Symposium National Irrigation Symposium, Phoenix, Arizona, 2000, pp. 401–408.
- [2] J. Li, Y. Meng, Y. Liu, Hydraulic performance of differential pressure tanks for fertigation, Trans. ASABE, 49 (2006) 1815–1822.
- [3] G.C. Karshner, Automatic Fertilizer, P.a.t. Office, Washington, U.S., 1932.
- [4] F. Thalasso, H. Naveau, E.-H. Nyns, Design and performance of a bioreactor equipped with a Venturi injector for high gas transfer rates, Chem. Eng. J. Biochem. Eng. J., 57 (1995) B1–B5.
- [5] J.S. Li, R.E. Yoder, L.O. Odhiambo, J. Zhang, Simulation of nitrate distribution under drip irrigation using artificial neural networks, Irrig. Sci., 23 (2004) 29–37.
- [6] F. Yoldas, S. Ceylan, B. Yagmur, N. Mordogan, Effects of nitrogen fertilizer on yield quality and nutrient content in broccoli, J. Plant Nutr., 31 (2008) 1333–1343.
- [7] S.T. Zodape, V.J. Kawarkhe, J.S. Patolia, A.D. Warade, Effect of liquid seaweed fertilizer on yield and quality of okra (*Abelmoschus esculentus* L.), J. Sci. Ind. Res., 67 (2008) 1115–1117.
- [8] R. Tognetti, M. Palladino, A. Minnocci, S. Delfine, A. Alvino, The response of sugar beet to drip and low-pressure sprinkler

- irrigation in southern Italy, *Agric. Water Manage.*, 60 (2003) 135–155.
- [9] L. Woltering, D. Pasternak, J. Ndjeunga, The African market garden: the development of a low-pressure drip irrigation system for smallholders in the sudano sahel, *Irrig. Drain.*, 60 (2011) 613–621.
- [10] A. Hamdy, R. Ragab, E. Scarascia-Mugnozza, Coping with water scarcity: water saving and increasing water productivity, *Irrig. Drain.*, 52 (2003) 3–20.
- [11] I. Papadopoulos, Micro-irrigation systems and fertigation, L.S. Pereira, R.A. Feddes, J.R. Gilley, B. Lesaffre, Eds., *Sustainability of Irrigated Agriculture*, Springer, Dordrecht, 1996, pp. 309–322.
- [12] I.E.L. Neto, R.D. Porto, Performance of low-cost ejectors, *J. Irrig. Drain. Eng.*, 130 (2004) 122–128.
- [13] Z. Yuan, C.Y. Choi, P.M. Waller, P. Colaizzi, Effects of liquid temperature and viscosity on Venturi injectors, *Trans. ASAE*, 43 (2000) 1441–1447.
- [14] J.D. Anderson, J. Wendt, *Computational Fluid Dynamics*, McGraw-Hill, New York, 1995.
- [15] B. Blocken, P. Moonen, T. Stathopoulos, J. Carmeliet, Numerical study on the existence of the Venturi effect in passages between perpendicular buildings, *J. Eng. Mech.*, 134 (2008) 1021–1028.
- [16] D.A. Ji, M.L. Zhang, T.G. Xu, K.Y. Wang, P.C. Li, F. Ju, Experimental and numerical studies of the jet tube based on venturi effect, *Vacuum*, 111 (2015) 25–31.
- [17] Z. Qiu, Simulation Study of Venturi Fertilizer Injector Based on Fluent, In: *Agricultural Bio-environment and Energy Engineering*, Southwest University, Chongqing, 2012 (in Chinese).
- [18] Y. Sun, Effects of Venturi Structural Parameters on the Absorption Fertilizer Performance, In: *Agricultural Soil and Water Engineering*, Northwest A&F University, Yangling, 2010 (in Chinese).
- [19] H. Yan, X. Chu, Numerical Simulation for Influence of Throat Diameter on Venturi Injector Performance, *J. Drain. Irrig. Mach. Eng.*, 29 (2011) 359–363 (in Chinese).
- [20] Y.J. Zhang, K.P. Liu, J.P. Liao, Y.D. Zhang, C.L. Wu, Y.C. Hu, Parameter Optimization of Multi-Stage Coilgun using Orthogonal Test Approach, 16th International Symposium on Electromagnetic Launch Technology, IEEE, Beijing, China, 2012.
- [21] L.J. Ji, Y.F. Si, H.F. Liu, X.L. Song, W. Zhu, A.P. Zhu, Application of orthogonal experimental design in synthesis of mesoporous bioactive glass, *Microporous Mesoporous Mater.*, 184 (2014) 122–126.
- [22] X. Wu, D.Y.C. Leung, Optimization of biodiesel production from camelina oil using orthogonal experiment, *Appl. Energy*, 88 (2011) 3615–3624.